Coexistent Diabetes Is Associated With the Presence of Adverse Phenotypic Features in Patients With Hypertrophic Cardiomyopathy

Nicholas Jex,[1] Amrit Chowdhary,[1] Sharmaine Thirunavukarasu,[1] Henry Procter,[2] Anshuman Sengupta,[2] Pavithra Natarajan,[1] Sindhoora Kotha,[1] Ana-Maria Poenar,[2] Peter Swoboda,[1] Hui Xue,[3] Richard M. Cubbon,[1] Peter Kellman,[3] John P. Greenwood,[1] Sven Plein,[1] Stephen Page,[2] and Eylem Levelt[1]

Diabetes Care 2022;45:1852–1862 | https://doi.org/10.2337/dc22-0083

OBJECTIVE

Type 2 diabetes mellitus (T2DM) is associated with worsened clinical outcomes in hypertrophic cardiomyopathy (HCM) patients. We sought to investigate whether HCM patients with T2DM comorbidity exhibit adverse cardiac alterations in myocardial energetics, function, perfusion, or tissue characteristics.

RESEARCH DESIGN AND METHODS

A total of 55 participants with concomitant HCM and T2DM (HCM-DM) ($n = 20$) or isolated HCM ($n = 20$) and healthy volunteers (HV) ($n = 15$) underwent ^{31}P-MRS and cardiovascular MRI. The HCM groups were matched for HCM phenotype.

RESULTS

Mean ± SD European Society of Cardiology sudden cardiac death risk scores were comparable between the HCM groups (HCM 2.2 ± 1.5%, HCM-DM 1.9 ± 1.2%; P = not significant), and sarcomeric mutations were equally common. HCM-DM patients had the highest median NT-proBNP levels (HV 42 ng/L [interquartile range 35–66], HCM 298 ng/L [157–837], HCM-DM 726 ng/L [213–8,695]; $P < 0.0001$). Left ventricular (LV) ejection fraction, mass, and wall thickness were similar between the HCM groups. HCM-DM patients displayed a greater degree of fibrosis burden with higher scar percentage and lower global longitudinal strain compared with HCM patients. PCr/ATP (the relative concentrations of phosphocreatine and ATP) was significantly lower in the HCM-DM group than in both HCM and HV (HV 2.17 ± 0.49, HCM 1.93 ± 0.38, HCM-DM 1.54 ± 0.27; $P = 0.002$). In a similar pattern, stress myocardial blood flow was significantly lower in the HCM-DM group than in both HCM and HV (HV 2.06 ± 0.42 mL/min/g, HCM 1.74 ± 0.44 mL/min/g, HCM-DM 1.39 ± 0.42 mL/min/g; $P = 0.002$).

CONCLUSIONS

We show for the first time that HCM-DM patients display greater reductions in myocardial energetics, perfusion, and contractile function and higher myocardial scar burden and serum NT-proBNP levels compared with patients with isolated HCM despite similar LV mass and wall thickness and presence of sarcomeric mutations. These adverse phenotypic features may be important components of the adverse clinical manifestation attributable to a combined presence of HCM and T2DM.

[1]Multidisciplinary Cardiovascular Research Centre and Biomedical Imaging Science Department, Leeds Institute of Cardiovascular and Metabolic Medicine, University of Leeds, Leeds, U.K.
[2]Department of Cardiology, Leeds Teaching Hospitals NHS Trust, Leeds, U.K.
[3]National Heart, Lung, and Blood Institute, National Institutes of Health, U.S. Department of Health and Human Services, Bethesda, MD

Corresponding author: Eylem Levelt, e.levelt@leeds.ac.uk

Received 15 January 2022 and accepted 3 May 2022

This article contains supplementary material online at https://doi.org/10.2337/figshare.19896205.

Hypertrophic cardiomyopathy (HCM) is the most common inherited cardiomyopathy with a population prevalence of 1 in 500 (1,2). HCM is associated with sudden cardiac death and may lead to heart failure at any age, although significant heterogeneity in phenotypic expression exists (1,2). Type 2 diabetes mellitus (T2DM) occurs concomitantly in 9% of patients with HCM and is associated with worsened clinical manifestation of HCM (3,4). HCM patients with T2DM comorbidity (HCM-DM) were shown to have greater prevalence of diastolic dysfunction and pulmonary hypertension, higher New York Heart Association (NYHA) Class, lower exercise capacity, and higher long-term mortality rate (3). Although distinct pathological entities, HCM and T2DM were shown to share common features of impaired myocardial energetics (5–7), coronary microvascular dysfunction (8,9), and myocardial fibrosis (10–15) in previous studies with investigation of these conditions in isolation. The mechanisms for the adverse prognostic association between HCM and T2DM are incompletely understood but likely include the collective impact of HCM and T2DM on myocardial energy metabolism, perfusion, and the fibrotic process.

PCr/ATP (the relative concentrations of phosphocreatine and ATP) is a sensitive index of the energetic state of the myocardium (16) that can be measured noninvasively with ^{31}P-MRS. Moreover, cardiovascular magnetic resonance (CMR) allows comprehensive evaluation of myocardial structure, function, strain, tissue characteristics, fibrosis, and perfusion with excellent reproducibility (17,18). Using CMR, investigators in previous studies identified factors associated with adverse cardiovascular events and mortality in HCM patients, including replacement fibrosis on late gadolinium enhancement imaging (LGE) (19). In addition to replacement fibrosis assessed with LGE, CMR is also established as a tool for quantification of diffuse fibrosis in quantifying the extracellular volume fraction (ECV) with native T1 mapping (20).

Combining ^{31}P-MRS and CMR in an observational prospective case-control study, we sought to test the hypothesis that coexistent diabetes is associated with greater reductions in myocardial energetics and perfusion and higher scar burden in HCM.

RESEARCH DESIGN AND METHODS

This single-center observational prospective case-control study complied with the Declaration of Helsinki and was approved by the National Research Ethics Committee (reference no. 18/YH/0168). Informed written consent was obtained from each participant. The data will be shared on reasonable request to the corresponding author.

Participants

A total of 55 participants including 20 with isolated HCM, 20 with HCM-DM, and 15 healthy volunteers (HV) were prospectively recruited. Genetic screening was undertaken for all HCM patients for 21 genes. Diagnosis of HCM was based on the presence of unexplained left ventricular (LV) hypertrophy (maximum wall thickness $\geq$15 mm) (1). Anderson-Fabry disease was excluded in all male adult patients with presumed HCM with a blood test for plasma and leukocyte α-galactosidase A (21), except for patients from families with established genetic forms of HCM or for previously diagnosed mutation carriers. In women with a suspicion for the condition, GLA gene test is performed for exclusion.

Two routes were used for recruitment of the participants with HCM (Fig. 1, CONSORT diagram). Eligible HCM patients were recruited from the regional inherited cardiac conditions (ICC) clinic over 2 years during their routine clinical appointment (May 2019–May 2021) and from a local registry of 426 HCM patients followed by our regional ICC clinic. This list was prescreened by an independent investigator (P.N.) in a nonparticipant facing role. After each prospective block of five HCM-DM participants was successfully recruited and completed the study visit, our regional ICC registry was revisited for identifying isolated HCM patients meeting eligibility criteria as well as for matching to scanned HCM-DM patients for age, sex, European Society of Cardiology (ESC) risk score profile, and hypertension comorbidity (P.N.). This practice was repeated for each block of five patients four times over the 2 years while this study was conducted. All data were analyzed in a blinded fashion after the completion of the study (last participant last visit). The blinding methodology is described in *QUANTITATIVE ANALYSIS*.

HCM-DM patients had an established diagnosis of T2DM according to World Health Organization criteria and were free of known diabetes complications (22). HV were recruited from local golf clubs. Ethnicity group was self-reported by participants.

Exclusion Criteria

Patients with known coronary artery disease (CAD), cardiac surgery, tobacco smoking, amyloidosis, permanent atrial fibrillation (AF), moderate or above valvular heart disease, renal impairment (estimated glomerular filtration rate [eGFR] $<$30 mL/min/1.73 m^2), and contraindications to CMR were excluded. For the diabetes cohorts, patients with any other forms of diabetes than T2DM were excluded. The safety or feasibility of ^{31}P-MRS has not been assessed in patients with a pacemaker or implantable cardioverter defibrillator (ICD); consequently, ^{31}P-MRS is not licensed for scanning these cohorts. Therefore, patients with a pacemaker or ICD were deemed ineligible for the study.

Anthropometric Measurements

Height and weight were recorded, and BMI was calculated. Blood pressure was recorded as an average of three measures taken over 10 min (DINAMAP 1846 SX; Critikon). Twelve-lead electrocardiogram was recorded. A fasting blood sample was taken for assessments of full blood count, eGFR, lipid profile, HbA_{1c}, insulin, and *N*-terminal prohormone brain natriuretic peptide (NT-proBNP).

^{31}P-MRS

^{31}P-MRS was performed to obtain the PCr/ATP from a voxel placed in the midventricular septum, with subjects lying supine and a ^{31}P transmitter/receiver cardiac coil (Rapid Biomedical GmbH, Rimpar, Germany) placed over the heart, in the iso-center of the magnet on a 3.0 Tesla magnetic resonance system (Prisma; Siemens Healthineers, Erlangen, Germany), as previously described (23).

CMR

The CMR protocol (Supplementary Material, scan protocol figure) consisted of cine imaging with a steady-state free precession sequence, native pre- and postcontrast T1 mapping, stress and rest perfusion, and LGE.

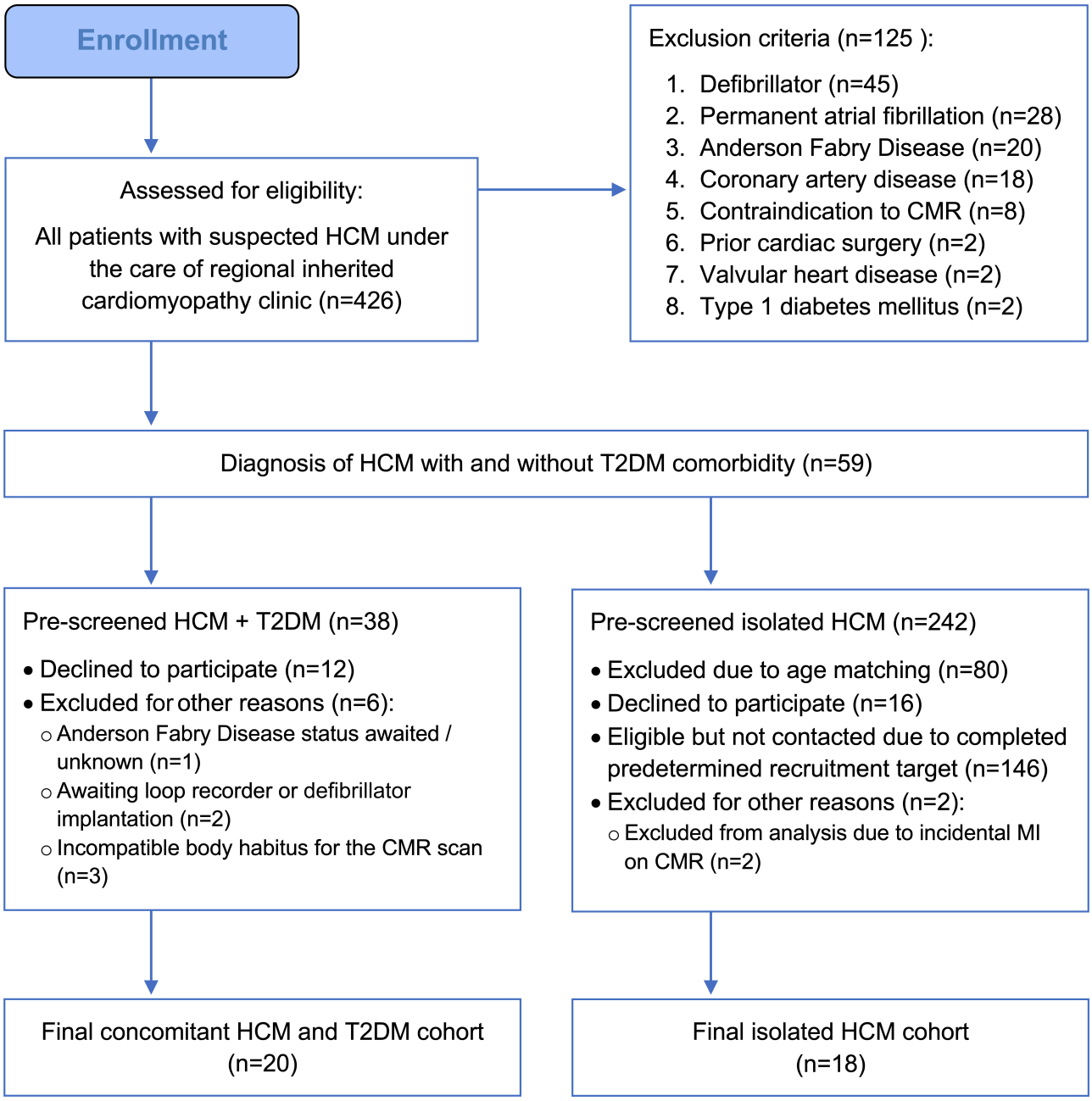

Figure 1—CONSORT flow diagram demonstrating the recruitment pathway for all study participants with HCM. MI, myocardial infarction.

Native T1 maps were acquired in three short-axis slices, including segments with maximal wall thickness, with use of a breath-held modified look-locker inversion recovery acquisition as previously described (23). Postcontrast T1 mapping acquisition was performed 15 min after last contrast injection.

Perfusion imaging used free-breathing, motion-corrected automated in-line perfusion mapping (18). Adenosine was infused at a rate of 140 μg/kg/min, increased to a maximum of 210 μg/kg/min according to hemodynamic and symptomatic response (a significant hemodynamic response was defined as >10 bpm increase in heart rate, or blood pressure drop >10 mmHg and one or more adenosine-related symptoms, e.g., chest tightness, breathlessness) (24). For perfusion imaging, an intravenous bolus of 0.05 mmol/kg gadobutrol (Gadovist, Leverkusen, Germany) was administered at 5 mL/s followed by a 20 mL saline flush with an injection pump (MEDRAD MRXperion Injection System; Bayer).

LGE was performed with a phase-sensitive inversion recovery sequence in LV short- and long-axis planes >8 min after contrast administration (25).

Quantitative Analysis

All ^{31}P-MRS analysis was performed off-line with blinding to participant details by N.J. after completion of the study using software within MATLAB version R2012a (MathWorks, Natick, MA) as previously described (26). The anonymization codes were only unlocked once all data analysis was completed.

All CMR image analysis, except for the scar percentage quantification on late gadolinium hyperenhancement imaging, was performed by N.J., and scan contours were subsequently reviewed by E.L., also blinded to participant details,

using cvi42 software (Circle Cardiovascular Imaging, Calgary, Canada). Images for biventricular volumes and function and LV maximal wall thickness were analyzed as previously described (27).

Left atrial (LA) volume and ejection fraction (EF) were calculated with the biplane area-length method in the horizontal and vertical long axes as previously described (28). Strain measurements were performed using cvi42 tissue tracking from the short axis images and the long axis views. Peak circumferential systolic strain, peak early diastolic strain rate, and global longitudinal strain (GLS) were measured (29).

Myocardial perfusion image reconstruction and processing were implemented using the Gadgetron software framework (18). Rest/stress myocardial blood flow (MBF) were measured for each of the 16 segments with use of the American Heart Association classification. T1 maps and ECV were analyzed with cvi42 software as previously described (15).

The LV short axis stack of late gadolinium hyperenhancement images was first assessed visually for presence of late gadolinium hyperenhancement, followed by quantification when late gadolinium hyperenhancement was present, as previously described (20). Late gadolinium hyperenhancement was defined as areas of signal intensity $\geq$5 SD from normal myocardium and was expressed as the percentage of LV mass, quantified in a blinded fashion.

Statistical Analysis

Statistical analysis was performed with GraphPad Prism software (version 9.0.0). Categorical data were compared with Pearson χ^2 test. All data were checked for normality with the Shapiro-Wilk test and are presented as means ± SD or median (interquartile range) as appropriate. Differences in continuous variables between the cohorts were assessed with one-way ANOVA with post hoc Bonferroni corrections. Differences in nonparametric variables were assessed with Kruskal-Wallis test. Student *t* test was used for comparison of normally distributed data sets, and Mann-Whitney *U* test was used for nonparametric tests where data were obtained for only two groups. *P* value of $\leq$0.05 was considered statistically significant.

Prespecified hypotheses were tested on three variables including myocardial PCr/ATP, stress MBF, and scar burden on late gadolinium hyperenhancement imaging.

Bivariate correlations were performed with use of Pearson correlation coefficient for parametric data or Spearman rank correlation coefficient for nonparametric data as appropriate.

The correlation analyses were performed to assess the associations between diabetes control (HbA_{1c}) and myocardial energetics (PCr/ATP) and between energetics and perfusion (myocardial perfusion reserve [MPR], global rest and stress MBF).

These correlation assessments were performed only for the HCM-DM group data. Additionally, these correlation assessments between the scar percentage and the perfusion parameters were performed for the combined data from the two HCM groups not including the HV data.

Priori sample size calculations were performed from the data acquired in T2DM patients before the study, which suggested that for detection of an 18% difference in the myocardial energetics (mean ± SD myocardial PCr/ATP in T2DM patients 1.74 ± 0.26, in control subjects 2.07 ± 0.35) (9), 14 participants per group across the three cohorts would be needed (with 80% power at α = 0.05). These recruitment goals were achieved in the study with 55 participants recruited.

There was only one patient in each HCM group with LV outflow tract gradient >30 mmHg at rest. Consequently, results were not adjusted for the presence of LV outflow tract gradient.

RESULTS

Participant Demographics and Clinical Characteristics

Demographics and clinical, genetic, and biochemical data are shown in Table 1. Of the 426 HCM patients screened from the local ICC clinic, 59 (14%) had a diagnosis of concomitant T2DM (Fig. 1). A total of 20 HCM-DM and 20 age- and sex-matched isolated HCM patients were prospectively recruited from clinics. Two isolated HCM patients were found to have previously undiagnosed silent myocardial infarction on CMR imaging and were excluded from the final analysis. In addition, 15 HV completed the study.

Participants across the three groups showed similar ethnicity distribution. The two HCM groups were matched for HCM phenotype (8 apical and 12 asymmetric septal hypertrophy in HCM-DM and 7 apical and 11 asymmetric septal hypertrophy in isolated HCM). There was no significant difference in ESC sudden cardiac death risk score (1) (HCM 2.2 ± 1.5%, HCM-DM 1.9 ± 1.2%; *P* = not significant), and an equal number of participants were confirmed with disease-causing sequence variants in sarcomeric protein genes between the two HCM groups (HCM 33%, HCM-DM 30%; *P* = not significant). Four HCM-DM and two HCM patients had a history of paroxysmal AF and two patients in each HCM group had a history of nonsustained ventricular tachycardia on 48-h ambulatory electrocardiogram monitoring. None of the patients in either HCM group had pediatric-onset HCM or had undergone alcohol septal ablation or myectomy. Reflecting the exclusion of participants receiving implantable cardioverter/defibrillators from the study to prevent unlicensed use of ^{31}P-MRS, none of the HCM participants had a previous history of sustained ventricular tachycardia or resuscitated cardiac arrest.

While the majority of isolated HCM patients described no exertional symptoms (83% NYHA class I, 17% class II, none class III or IV), 50% of the HCM-DM group were classified as NYHA class I, 45% NYHA class II, and 5% NYHA class III based on symptom status. In symptomatic patients with NYHA class II or above, obstructive CAD (>50% of luminal stenosis) was excluded within the last 5 years with invasive coronary angiography in eight HCM-DM and five HCM patients and with coronary computed tomographic angiography in one HCM-DM patient as part of routine clinical care.

None of the HCM patients had a history of cerebrovascular events, but four HCM-DM patients had this background. HV did not report exertional symptoms.

There were no significant differences in blood pressure or resting heart rate across the groups. The HCM and HCM-DM groups were matched for hypertension comorbidity. As more participants in the HCM-DM group was receiving statin treatment, the LDL cholesterol levels were lower in the HCM-DM group than in HV and HCM.

Table 1—Clinical characteristics and biochemistry

	HV (*n* = 15)	HCM (*n* = 18)	HCM-DM (*n* = 20)	*P*
Age, years	60 ± 12	59 ± 10	64 ± 9	0.25
Female	5 (33)	4 (22)	7 (35)	0.39
White	10 (67)	12 (67)	12 (60)	0.74
South Asian	4 (27)	5 (28)	7 (35)	0.67
BMI, kg/m^2	25 ± 3¶	29 ± 5	32 ± 6	**0.0003**
Heart rate, bpm	64 ± 11	62 ± 15	69 ± 14	0.11
Systolic BP, mmHg	134 ± 19	123 ± 13	133 ± 18	0.13
Diastolic BP, mmHg	76 ± 8	77 ± 6	76 ± 7	0.91
Creatinine, μmol/L	73 ± 10	81 ± 14	77 ± 19	0.23
eGFR, ml/min/1.73m^2	83 ± 8	79 ± 9	78 ± 15	0.39
Total cholesterol, mmol/L	5.3 ± 1.1¶	5.3 ± 1.2€	3.8 ± 0.7	**<0.0001**
HDL, mmol/L	1.7 ± 0.4¶	1.5 ± 0.3	1.2 ± 0.2	**<0.0001**
LDL, mmol/L	2.9 ± 0.9¶	3.1 ± 1.1€	1.9 ± 0.6	**0.0005**
TG, mmol/L	1.3 ± 0.6	1.5 ± 0.7	1.6 ± 0.5	0.48
HbA_{1c}, mmol/mol	37 ± 3¶	36 ± 3€	56 ± 7	**<0.0001**
Insulin, pmol/L	35 ± 25¶	53 ± 48€	139 ± 136	**0.001**
NT-proBNP, ng/L	42 (35–66)¶†	298 (157–837)	725 (213–2,006)	**<0.0001**
ACEi		2 (11)	9 (45)	**0.01**
ARB		2 (11)	2 (10)	0.91
β-Blocker		7 (39)	12 (60)	0.32
CCB		5 (28)	8 (40)	0.36
Statin		4 (22)	17 (85)	**0.0001**
ASA		0 (0)	3 (17)	0.08
DOAC		1 (6)	4 (20)	0.19
Metformin			15 (75)	0.1
Sulfonylurea			1 (5)	0.29
DPP-4i			3 (15)	0.68
GLP-1RA			1 (5)	0.31
SGLT2i			5 (25)	0.08
Genotype positive		6 (33)	6 (30)	0.83
MYH7		4 (22)	2 (10)	
MYBPC3		2 (11)	1 (5)	
ACTC1		0 (0)	1 (5)	
TNNI3		0 (0)	1 (5)	
Phenotype				
Asymmetric septal hypertrophy		11 (61)	12 (60)	0.94
Apical hypertrophy		7 (39)	8 (40)	0.94
NSVT		2 (11)	2 (10)	0.91
NYHA class				
I		15 (83)	10 (50)	**0.03**
II		3 (17)	9 (45)	0.06
III		0 (0)	1 (5)	0.34
IV		0 (0)	0 (0)	
ESC risk score, %		2.2 ± 1.5	1.9 ± 1.2	0.57
Syncope		1 (6)	1 (5)	0.94
Family history of SCD		2 (11)	1 (5)	0.49

Continued on p. 1857

Table 1—Continued

	HV (n = 15)	HCM (n = 18)	HCM-DM (n = 20)	P
Stroke TIA		0 (0)	4 (20)	**0.04**
HTN		6 (33)	8 (40)	0.3
PAF		2 (11)	4 (20)	0.45

Data are n (%), median (interquartile range), or mean ± SD. ACEI, ACE inhibitor; ACTC1, actin α cardiac muscle 1; ARB, angiotensin receptor blocker; ASA, aspirin; BP, blood pressure; CCB, calcium channel blocker; DOAC, direct oral anticoagulant; DPP-4i, dipeptidyl peptidase 4 inhibitor; GLP-1RA, glucagon-like peptide 1 receptor agonist; HTN, hypertension; MYBPC3, myosin binding protein C; MYHY7, myosin heavy chain 7; NSVT, nonsustained ventricular tachycardia; PAF, paroxysmal AF; SCD, sudden cardiac death; SGLT2i, SGLT2 inhibitor; TIA, transient ischemic attack; TG, triglycerides; TNNI3, troponin I. €$P < 0.05$ between HCM-DM and HCM with Bonferroni correction; ¶$P < 0.05$ between HCM-DM and HV with Bonferroni correction; †$P \leq 0.05$ between HCM and HV with Bonferroni correction. Boldface indicates statistically significant P value.

There was a stepwise increase in median NT-proBNP levels in the order of smallest measurements to greatest, respectively (HV 42 ng/L [interquartile range 35–66], HCM 298 ng/L [157–837], HCM-DM 726 ng/L [213–8695]; $P < 0.0001$), with significant increases in both HCM groups compared with HV.

Cardiac Geometry and Function

CMR/^{31}P-MRS results are shown in Table 2. The HCM groups were comparable in LV volumes, mass, and EF, with no significant difference in maximal LV wall thickness between the two groups. As expected, LV EF, mass, and wall thickness were significantly higher in the HCM groups compared with HV.

HCM-DM patients showed greater LV concentricity with a higher LV mass–to–LV end-diastolic volume ratio compared with HV and HCM (Supplementary Material). Comorbidity with T2DM was associated with greater reductions in GLS ($P < 0.002$), peak systolic circumferential strain ($P = 0.0005$), and diastolic strain ($P = 0.002$) rate.

There was no significant difference in mean ± SD LA volumes across the groups, but there was a stepwise decline in LA EF in the order of greatest measurements to smallest: HV 62 ± 7%, HCM 45 ± 10%, HCM-DM 34 ± 18%; $P < 0.0001$.

None of the participants with HCM showed a reduction in noncontrast T1 signal or a characteristic pattern of hyperenhancement on LGE suggestive of Anderson-Fabry disease (30,31).

Myocardial Energetics

HCM-DM patients showed significant reductions in mean ± SD PCr/ATP compared with HV and HCM patients (HV 2.17 ± 0.49, HCM 1.93 ± 0.38, HCM-DM 1.54 ± 0.27; $P = 0.002$). The numeric differences in PCr/ATP between the isolated HCM patients and HV were not statistically significant.

Five HCM-DM patients were on sodium–glucose cotransporter 2 (SGLT2) inhibitors. The myocardial PCr/ATP for the HCM-DM patients on SGLT2 inhibitors (1.55, 95% CI 1.00–1.85) was separately measured.

Myocardial Perfusion

Changes in rate pressure product (RPP) from rest to stress and rest and stress MBF and MPR measurements are summarized in Table 2, with representative images from each group in Fig. 2. Participants from all groups demonstrated a similar increase in RPP during adenosine stress.

There was again a stepwise decline in mean ± SD stress MBF in the order of greatest measurements to smallest (HV 2.06 ± 0.42 mL/min/g, HCM 1.74 ± 0.44 mL/min/g, HCM-DM 1.39 ± 0.42 mL/min/g; $P = 0.002$), with significant reductions in the HCM-DM group compared with the other two groups.

The stress MBF was not significantly reduced in the isolated HCM group compared with HV. The rest MBF values were comparable across the groups. MPR was also only significantly reduced in the HCM-DM group compared with the other groups.

Myocardial Fibrosis and Scar Burden

Presence of midwall hyperenhancement in a nonischemic pattern was detected in all HCM patients and none of the HV (Supplementary Material). Two isolated HCM patients showed evidence of subendocardial hyperenhancement confirming the presence of a silent chronic myocardial infarction. All of their results were excluded from final analysis.

Comorbidity with T2DM was associated with greater mean ± SD myocardial scar percentage on LGE in the HCM patients (HCM 4 ± 4% vs. HCM-DM 10 ± 8%; $P = 0.002$).

While the precontrast native T1 map measurements were comparable across the groups, median myocardial ECV measurements were significantly higher for the HCM groups (HV 25% [interquartile range 23–26], HCM 27% [22–31], HCM-DM 31% [27–43]; $P = 0.006$) (Supplementary Material).

Comparison of the Principal Study Findings Between the HCM Patients With and Without T2DM

In addition to the myocardial scar percentage comparisons on the LGE, direct comparisons of the principal findings between the two HCM groups were also performed separately. These confirmed significantly higher scar percentage of the LV mass, and significantly lower GLS, myocardial PCr/ATP, and global stress MBF and MPR, in the HCM-DM group than in the HCM group (Fig. 3).

Correlations

A correlation between the stress MBF and myocardial scar percentage was detected in the two HCM groups ($r = -0.459$, $P = 0.01$). There was no significant correlation between HbA_{1c} and PCr/ATP in the isolated data from the HCM-DM group ($r = -0.4417$, $P = 0.1$). There were no significant correlations between the rest or stress MBF and PCr/ATP.

CONCLUSIONS

Coexistence of T2DM is associated with worsened clinical manifestation of HCM (3,4). The current study provides insights into this prognostic association by showing

Table 2—CMR and ^{31}P-MRS findings

	HV (n = 15)	HCM (n = 18)	HCM-DM (n = 20)	P
LV end-diastolic volume indexed to BSA, mL/m^2	83 ± 18	82 ± 19	76 ± 22	0.08
LV end-systolic volume indexed to BSA, mL/m^2	31 ± 7¶	28 ± 15	26 ± 14	**0.02**
LV mass, g	99 ± 27¶†	173 ± 63	187 ± 73	**<0.0001**
LV mass index, g/m^2	54 ± 11¶†	90 ± 27	92 ± 40	**<0.0001**
LV mass to LV end diastolic volume ratio, g/mL	0.65 ± 0.11¶	1.03 ± 0.31	1.24 ± 0.36	**<0.0001**
LV stroke volume, mL	95 ± 23†	118 ± 21	101 ± 22	**0.01**
LV ejection fraction, %	63 ± 4†	70 ± 9	67 ± 9	**0.04**
LV maximal wall thickness, mm	10 ± 1¶†	20 ± 2	21 ± 4	**<0.0001**
RV end-diastolic volume indexed to BSA, mL/m^2	86 ± 20¶	79 ± 14€	66 ± 13	**0.001**
RV end-systolic volume indexed to BSA, mL/m^2	35 ± 10	30 ± 10	28 ± 13	0.23
RV stroke volume, mL	95 ± 23¶	94 ± 16€	75 ± 21	**0.008**
RV ejection fraction, %	60 ± 6	62 ± 8	58 ± 13	0.42
LA biplane end-systolic volumes, mL	67 ± 17¶†	100 ± 28	113 ± 59	**0.0008**
Biplane LA EF, %	62 ± 7¶†	45 ± 10	34 ± 18	**<0.0001**
GLS negative, %	14 ± 3¶	13 ± 3€	10 ± 4	**0.002**
Peak systolic circumferential strain negative, %	21 ± 2¶	20 ± 4€	16 ± 4	**0.0005**
Peak circumferential diastolic strain rate, s^{-1}	1.19 ± 0.24¶	0.99 ± 0.21	0.87 ± 0.22	**0.002**
Mean native T1, ms	1,211 ± 81	1,211 ± 65	1,209 ± 69	0.99
Extracellular volume, %	25 (23–26)¶	27 (22–29)€	31 (27–43)	**0.006**
LGE scar percentage of LV mass, %		4 ± 4	10 ± 8	**0.007**
PCr/ATP	2.17 ± 0.49¶	1.93 ± 0.38€	1.54 ± 0.27	**0.002**
Increase in RPP, %	37	33	32	0.3
Stress MBF, mL/min/g	2.06 ± 0.42¶	1.74 ± 0.44€	1.39 ± 0.42	**0.002**
Rest MBF, mL/min/g	0.68 ± 0.03	0.59 ± 0.19	0.69 ± 0.16	0.05
MPR	3.19 ± 0.79¶	3.09 ± 1.06€	2.04 ± 0.82	**0.002**

Data are means ± SD or median (interquartile range) unless otherwise indicated. BSA, body surface area; RV, right ventricle. €$P < 0.05$ between HCM-DM and HCM with Bonferroni correction; ¶$P < 0.05$ between HCM-DM and HV with Bonferroni correction; †$P \leq 0.05$ between HCM and HV with Bonferroni correction. Boldface indicates statistically significant P value.

adverse cardiac alterations in myocardial energetics, function, perfusion, and tissue characteristics in patients with T2DM and HCM comorbidity. It is the first prospective case-control study comparing groups of HCM patients with and without T2DM, carefully matched in HCM phenotype, LV mass, maximal wall thickness, presence of sarcomeric mutations, and the ESC sudden cardiac death risk score.

The results of the current study provide several new findings. First, one-half of the HCM-DM patients described exertional symptoms, were accordingly classified as NYHA class II or higher, and had significantly increased NT-proBNP levels compared with the HCM group, the majority of whom described no exertional symptoms and were NYHA class I. Second, HCM-DM patients displayed a greater burden of myocardial fibrosis than HCM patients. Third, reductions in stress MBF and MPR were more pronounced in HCM-DM patients than in patients with either disease alone. We detected amplified alterations in PCr/ATP in the HCM-DM group compared with the HCM group. Finally, HCM-DM patients displayed greater reductions in strain parameters and LA function compared with HCM patients. Taken together, while these findings suggest that combined presence of HCM and T2DM may adversely affect the phenotypic expression of HCM, as well as symptom status and plasma biomarkers such as NT-proBNP, our data cannot prove a causal link, in line with the cross-sectional observational nature of the study design. The causality of this relationship will need to be investigated in future studies.

This study is limited by a relatively small sample size, in line with its proof-of-principle nature and strict inclusion/exclusion criteria to ensure rigorous matching of the HCM cohorts in HCM phenotype, ESC risk score, and presence of sarcomeric mutations. However, using the large data set of the EURObservational Research Programme (EORP) Cardiomyopathy Registry of 1,739 patients with HCM, Lopes et al. (32) analyzed the relation of hypertension, T2DM, BMI, and clinical traits. They showed the prevalence of hypertension, T2DM, and obesity was 37%, 10%, and 21%, respectively. In our regional ICC

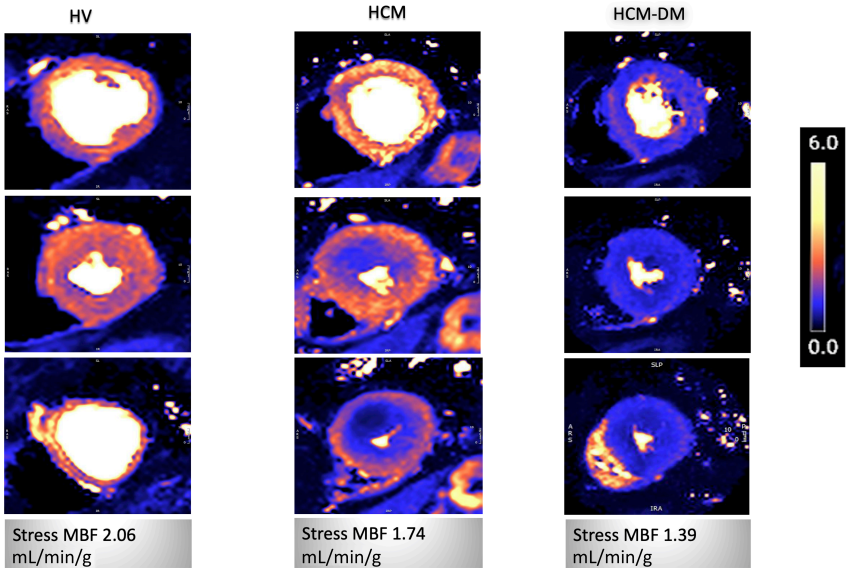

Figure 2—Representative examples of midleft ventricular stress perfusion maps from an HV, a patient with HCM, and a patient with HCM-DM.

registry, prevalence of T2DM is higher, at 14%, broadly in line with the higher T2DM prevalence in the local population of Yorkshire compared with the rest of the U.K. (33). In line with our findings, Lopes et al. showed that T2DM was associated with higher NYHA class and diastolic dysfunction.

Elevated NT-proBNP concentrations were shown to be a strong predictor of overall prognosis in patients with HCM (34). In a recent retrospective study, Wang et al. (35) reported outcomes of HCM patients with T2DM comorbidity undergoing septal myectomy over a median of 28 years' follow-up. They showed that while HCM patients with and without T2DM have similar 3-year cardiovascular mortality after septal myectomy, there was an association between T2DM comorbidity and the higher sudden cardiac death rate in these patients. While we have excluded patients undergoing septal myectomy in this study, potentially relevant for our findings of higher NT-proBNP levels in HCM-DM patients, they showed that NT-proBNP was an independent risk factor in their cohort of HCM patients with T2DM comorbidity.

In this study, 33% of the HCM and 30% of the HCM-DM group were genotype positive for sarcomeric mutations. While early studies from specialist referral centers had suggested that most individuals with HCM (>60%) carried a mutant sarcomere protein, in line with our findings, a large international registry study (Hypertrophic Cardiomyopathy Registry [HCMR]) showed genotype-negative cases to be the majority (36,37). The participants in the isolated HCM group in this study showed similarities with the HCMR cohort in demographic and clinical characteristics (mean ± SD age 59 ± 10 vs. 49 ± 11 years, male participant proportion 78% vs. 71%, ESC risk score 1.9 ± 1.2 vs, 2.48 ± 0.56, maximal wall thickness 20 ± 2 vs. 20.6 ± 4.8 mm, LV mass–to–end-diastolic volume ratio 1.03 ± 0.31 vs. 1.0 ± 0.3, scar percentage of the LV mass on LGE 4 ± 4% vs. 3.7 ± 5.2%, respectively), suggesting that the isolated HCM group in this study can be considered largely representative of the wider HCM population (36).

A previous study had shown higher prevalence of T2DM comorbidity in patients with an apical HCM phenotype compared with nonapical HCM phenotypes, although the reasons for this are not well understood (3). Supporting this, the prevalence of apical phenotype was higher in our regional ICC clinic HCM cohort among patients with T2DM comorbidity. However, in this study HCM cohorts were carefully matched in HCM phenotypes to prevent potential biases related to HCM variant differences.

A recent study investigated whether genetic variants may contribute to a combined phenotype of HCM and T2DM (38) showing predominant presence of gain-of-function variants in adiponectin receptor ADIPOR1 in HCM patients with T2DM comorbidity. ADIPOR1 plays a prominent role in mediating the insulin-sensitizing effects of adiponectin. Of potential significant relevance to our finding of greater reductions in myocardial energetics in HCM-DM patients, the deletion of ADIPOR1 was shown to result in decreased AMP-activated protein activity and the induction of mitochondrial dysfunction (38).

Underscoring the links between early exposure to the diabetic milieu and fetal myocardial structural and functional alterations, elevated neonatal IGF-I levels were shown to be associated with fetal HCM phenotype in fetuses of women with gestational diabetes mellitus (39).

Despite being shown to be predictors of adverse clinical outcomes including arrhythmic events and mortality in HCM (19,40), myocardial fibrosis and reductions in myocardial perfusion are not yet included among the criteria of existing risk scores. We have identified greater reductions in myocardial perfusion and higher scar burden in HCM-DM patients. It was proposed that T2DM-associated endothelial inflammation and profibrotic signaling may exacerbate the pathological hypertrophic remodeling in HCM and worsen coronary microvascular function (10,41–43). Our findings of greater reductions in stress MBF and MPR in HCM-DM support this theory. In support of the theory that myocardial ischemia caused by coronary microvascular dysfunction in HCM leads to enhanced scarring (8), we detected significant correlations between the myocardial LGE percentage and the stress MBF in the HCM groups.

Although prognostic data related to an impaired energetic state in HCM are lacking, it is believed to hold prognostic relevance in analogy to patients with dilated cardiomyopathy (44). It has been suggested that the high incidence of exercise-related death in HCM may be explained by a possible further acute impairment of myocardial energetics resulting in ion-pump dysfunction, calcium overload, and ventricular arrhythmias (7). Supporting this, exacerbation of myocardial energetic compromise has been documented in HCM patients during exercise activity (7). The correlation analyses were performed to assess the associations between diabetes control (HbA_{1c}) and myocardial energetics (PCr/

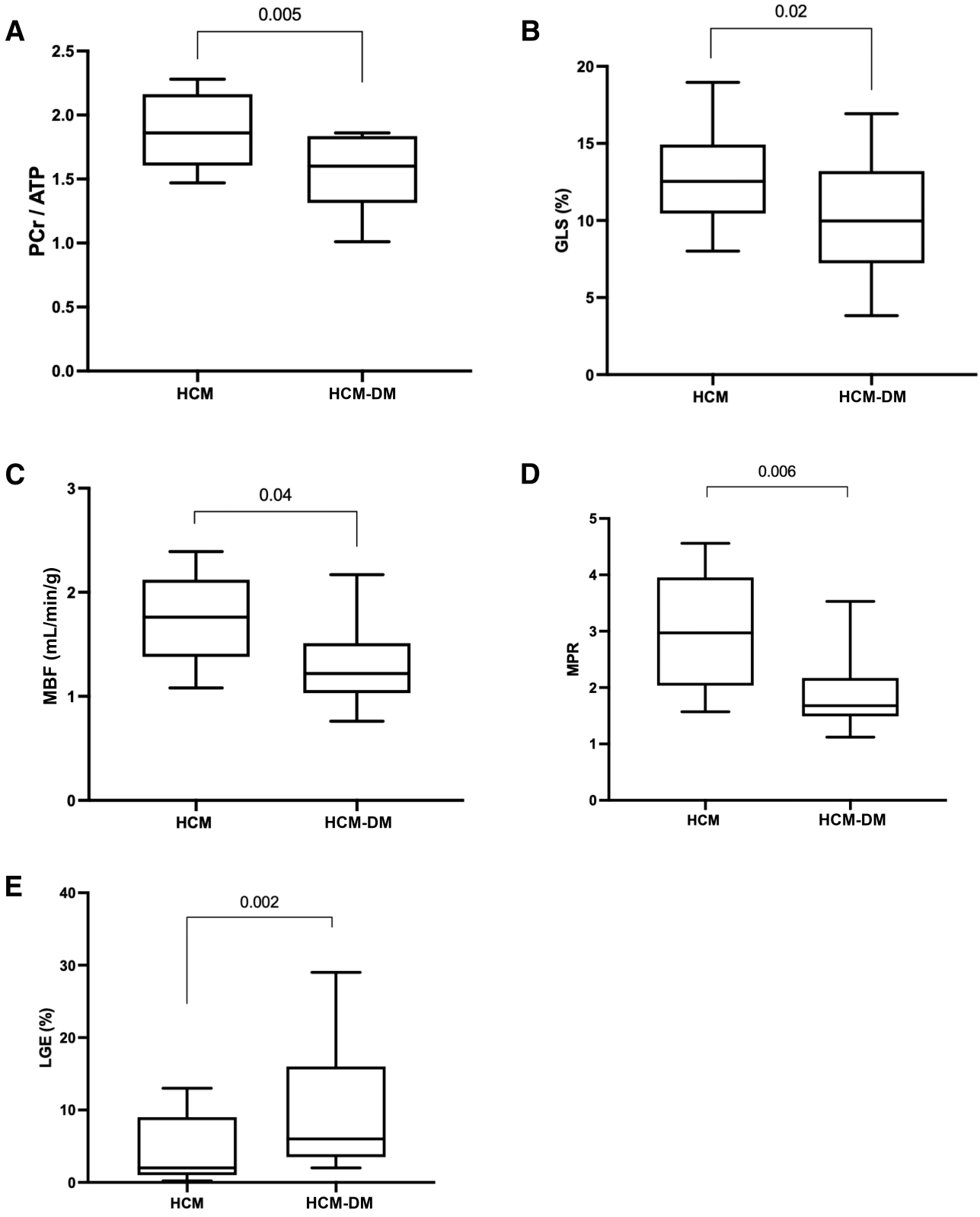

Figure 3—Differences in myocardial PCr/ATP, LV GLS, MPR, and global stress myocardial bloods flow and scar percentage between HCM and HCM-DM groups. Box and whisker plots show geometric mean, 25th and 75th percentiles, and the minimum to maximum data. Myocardial PCr/ATP (*A*), LV GLS (%) (*B*), global stress MBF (mL/min/g) (*C*), MPR (*D*), and myocardial scar percentage on LGE imaging between the two HCM groups where scar was present (%) (*E*).

ATP) only within the HCM-DM group and did not show significance. Larger studies of patients with concomitant diabetes and HCM are needed for assessment of this relationship.

With regard to comparison of the functional changes, GLS derived from either speckle tracking echocardiography or CMR is a sensitive marker of LV contractile function, especially in the setting of a normal LV EF (45). A recent meta-analysis of HCM studies showed an association of abnormal GLS with adverse composite cardiovascular outcomes and ventricular arrhythmias (45). In our study across the four groups, HCM-DM patients showed the greatest reductions in GLS. Moreover, while LV circumferential strain is also a sensitive index of regional myocardial function, currently, no studies have assessed its prognostic value in HCM or T2DM populations.

While the prognostic role of changes in LA size is established in patients with HCM and increased LA diameter correlates with occurrence of AF in patients with HCM, the prognostic role of LA function has not yet been explored in longitudinal studies. In our study, while the LA size was comparable between the two HCM cohorts, HCM-DM patients showed significant reductions in LA EF, which may be relevant for future risk of AF occurrence and thromboembolic events. Future studies are needed to explore this.

Limitations

This study is limited by the small sample size. The ^{31}P-MRS technique is not licensed for scanning patients with a pacemaker or an ICD; therefore, HCM patients with these devices had to be excluded from the study. The midseptal voxel is the most reproducible cardiac voxel for ^{31}P-MRS (46,47). Recruiting participants who underwent alcohol septal ablation or septal myectomy could therefore lead to iatrogenic abnormalities in the spectroscopy findings. Therefore, patients who have undergone these procedures had to be excluded from the study. However, the HCM groups were matched for HCM phenotype, with similar numbers for apical or asymmetric septal hypertrophy subgroups.

The study is also limited by the high prevalence of apical HCM, which means the results may be affected by selection bias and may not be generalizable to the wider population with HCM.

There remain potentially important differences between the HCM and HCM-DM groups with respect to age and sex. Due to the small sample size, other potentially important differences between groups, e.g., concomitant medication, cannot be accounted for. The matching of ESC risk score may have introduced additional unexpected confounding.

Obstructive CAD was excluded within the last 5 years as part of routine clinical care in all symptomatic HCM patients who were NYHA class II or above. For prevention of unnecessary ionizing radiation exposure, these tests were not repeated for the study. Therefore, it is possible that occult CAD could be present in the participants.

Conclusion

Coexistent diabetes is associated with higher NT-proBNP levels; greater reductions in myocardial energetics, perfusion, contractile function, and LA function; and higher scar burden in patients with HCM. These adverse phenotypic features may be important components of the adverse clinical manifestation attributable to a combined presence of HCM and T2DM.

Acknowledgments. The authors thank Emma Josephine, Levelt, U.K., for contributions to the structured graphical abstract design.

Funding. This study was supported by the Wellcome Trust (grant 207726/Z/17/Z). N.J. receives support from Diabetes U.K. (grant 18/0005908, Diabetes U.K. PhD studentship). E.L. is funded by a Wellcome Trust Clinical Career Development Fellowship (grant 221690/Z/20/Z). A.C. receives support from the British Heart Foundation (grant FS/CRTF/20/24003). The funders had no role in study design, data collection and analysis, decision to publish, or preparation of the manuscript.

Duality of Interest. No potential conflicts of interest relevant to this article were reported.

Author Contributions. N.J. contributed to subject recruitment; data acquisition, analysis, and interpretation; and drafting of the manuscript and revisions. A.C., S.T., H.P., P.N., and A.-M.P. contributed to data analysis and interpretation and manuscript revision. A.S., S.K., P.S., H.X., R.M.C., P.K., J.P.G., S.Pl., and S.Pa. contributed to data interpretation and manuscript revision. E.L. contributed to study conception and design; data acquisition, analysis, and interpretation; drafting of the manuscript and revisions; and study supervision. E.L. is the guarantor of this work and, as such, had full access to all the data in the study and takes responsibility for the integrity of the data and the accuracy of the data analysis.

References

1. Elliott PM, Anastasakis A, Borger MA, et al.; Authors/Task Force members. 2014 ESC guidelines on diagnosis and management of hypertrophic cardiomyopathy: the Task Force for the Diagnosis and Management of Hypertrophic Cardiomyopathy of the European Society of Cardiology (ESC). Eur Heart J 2014;35:2733–2779
2. Maron BJ, Gardin JM, Flack JM, Gidding SS, Kurosaki TT, Bild DE. Prevalence of hypertrophic cardiomyopathy in a general population of young adults. Echocardiographic analysis of 4111 subjects in the CARDIA Study. Coronary Artery Risk Development in (Young) Adults. Circulation 1995;92:785–789
3. Wasserstrum Y, Barriales-Villa R, Fernández-Fernández X, et al. The impact of diabetes mellitus on the clinical phenotype of hypertrophic cardiomyopathy. Eur Heart J 2019;40:1671–1677
4. Liu Q, Li D, Berger AE, Johns RA, Gao L. Survival and prognostic factors in hypertrophic cardiomyopathy: a meta-analysis. Sci Rep 2017;7:11957
5. Shivu GN, Phan TT, Abozguia K, et al. Relationship between coronary microvascular dysfunction and cardiac energetics impairment in type 1 diabetes mellitus. Circulation 2010;121:1209–1215
6. Scheuermann-Freestone M, Madsen PL, Manners D, et al. Abnormal cardiac and skeletal muscle energy metabolism in patients with type 2 diabetes. Circulation 2003;107:3040–3046
7. Dass S, Cochlin LE, Suttie JJ, et al. Exacerbation of cardiac energetic impairment during exercise in hypertrophic cardiomyopathy: a potential mechanism for diastolic dysfunction. Eur Heart J 2015;36:1547–1554
8. Petersen SE, Jerosch-Herold M, Hudsmith LE, et al. Evidence for microvascular dysfunction in hypertrophic cardiomyopathy: new insights from multiparametric magnetic resonance imaging. Circulation 2007;115:2418–2425
9. Levelt E, Rodgers CT, Clarke WT, et al. Cardiac energetics, oxygenation, and perfusion during increased workload in patients with type 2 diabetes mellitus. Eur Heart J 2016;37:3461–3469
10. Olivotto I, Girolami F, Sciagrà R, et al. Microvascular function is selectively impaired in patients with hypertrophic cardiomyopathy and sarcomere myofilament gene mutations. J Am Coll Cardiol 2011;58:839–848
11. Timmer SA, Germans T, Götte MJ, et al. Determinants of myocardial energetics and efficiency in symptomatic hypertrophic cardiomyopathy. Eur J Nucl Med Mol Imaging 2010;37:779–788
12. Toepfer CN, Garfinkel AC, Venturini G, et al. Myosin sequestration regulates sarcomere function, cardiomyocyte energetics, and metabolism, informing the pathogenesis of hypertrophic cardiomyopathy. Circulation 2020;141:828–842
13. Joy G, Crane JD, Lau C, et al. Impact of obesity on myocardial microvasculature assessed using fully-automated inline myocardial perfusion mapping CMR. Eur Heart J Cardiovascular Imaging 2021; 22 (Suppl. 1):jeaa35.296
14. Levelt E, Gulsin G, Neubauer S, McCann GP. Mechanisms in endocrinology: diabetic cardio-

myopathy: pathophysiology and potential metabolic interventions state of the art review. Eur J Endocrinol 2018;178:R127–R139
15. Swoboda PP, McDiarmid AK, Erhayiem B, et al. Diabetes mellitus, microalbuminuria, and subclinical cardiac disease: identification and monitoring of individuals at risk of heart failure. J Am Heart Assoc 2017;6:e005539
16. Neubauer S. The failing heart–an engine out of fuel. N Engl J Med 2007;356:1140–1151
17. Moon JC, Treibel TA, Schelbert EB. T1 mapping for diffuse myocardial fibrosis: a key biomarker in cardiac disease? J Am Coll Cardiol 2013;62:1288–1289
18. Kellman P, Hansen MS, Nielles-Vallespin S, et al. Myocardial perfusion cardiovascular magnetic resonance: optimized dual sequence and reconstruction for quantification. J Cardiovasc Magn Reson 2017;19:43
19. O'Hanlon R, Grasso A, Roughton M, et al. Prognostic significance of myocardial fibrosis in hypertrophic cardiomyopathy. J Am Coll Cardiol 2010;56:867–874
20. Treibel TA, Kozor R, Schofield R, et al. Reverse myocardial remodeling following valve replacement in patients with aortic stenosis. J Am Coll Cardiol 2018;71:860–871
21. Authors/Task Force members; Elliott PM, Anastasakis A, Borger MA, et al. 2014 ESC guidelines on diagnosis and management of hypertrophic cardiomyopathy: the Task Force for the Diagnosis and Management of Hypertrophic Cardiomyopathy of the European Society of Cardiology (ESC). Eur Heart J 2014;35:2733–2779
22. Alberti KG, Zimmet PZ. Definition, diagnosis and classification of diabetes mellitus and its complications. Part 1: diagnosis and classification of diabetes mellitus provisional report of a WHO consultation. Diabet Med 1998;15:539–553
23. Thirunavukarasu S, Jex N, Chowdhary A, et al. Empagliflozin treatment is associated with improvements in cardiac energetics and function and reductions in myocardial cellular volume in patients with type 2 diabetes. Diabetes 2021;70:2810–2822
24. Kramer CM, Barkhausen J, Flamm SD, Kim RJ, Nagel E, Society for Cardiovascular Magnetic Resonance Board of Trustees Task Force on Standardized Protocols. Standardized cardiovascular magnetic resonance (CMR) protocols 2013 update. J Cardiovasc Magn Reson 2013;15:91
25. Treibel TA, Kozor R, Menacho K, et al. Left ventricular hypertrophy revisited: cell and matrix expansion have disease-specific relationships. Circulation 2017;136:2519–2521
26. Purvis LAB, Clarke WT, Biasiolli L, et al. OXSA: An open-source magnetic resonance spectroscopy analysis toolbox in MATLAB. PLoS One 2017; Sep 22;12(9):e0185356. DOI: 10.1371/journal.pone.0185356
27. Rider OJ, Lewandowski A, Nethononda R, et al. Gender-specific differences in left ventricular remodelling in obesity: insights from cardiovascular magnetic resonance imaging. Eur Heart J 2013;34:292–299
28. Hudsmith LE, Petersen SE, Tyler DJ, et al. Determination of cardiac volumes and mass with FLASH and SSFP cine sequences at 1.5 vs. 3 Tesla: a validation study. J Magn Reson Imaging 2006;24:312–318
29. Gulsin GS, Swarbrick DJ, Hunt WH, et al. Relation of aortic stiffness to left ventricular remodeling in younger adults with type 2 diabetes. Diabetes 2018;67:1395–1400
30. Sado DM, White SK, Piechnik SK, et al. Identification and assessment of Anderson-Fabry disease by cardiovascular magnetic resonance noncontrast myocardial T1 mapping. Circ Cardiovasc Imaging 2013;6:392–398
31. Karur GR, Robison S, Iwanochko RM, et al. Use of myocardial T1 mapping at 3.0 T to differentiate Anderson-Fabry disease from hypertrophic cardiomyopathy. Radiology 2018;288:398–406
32. Lopes LR, Losi M-A, Sheikh N, et al.; Cardiomyopathy Registry Investigators Group. Association between common cardiovascular risk factors and clinical phenotype in patients with hypertrophic cardiomyopathy from the European Society of Cardiology (ESC) EurObservational Research Programme (EORP) Cardiomyopathy/Myocarditis Registry. Eur Heart J Qual Care Clin Outcomes. 9 February 2022. DOI: 10.1093/ehjqcco/qcac006
33. Population estimates. Office for National Statistics, 2021. Accessed 2 March 2022. Available from https://www.ons.gov.uk/peoplepopulationandcommunity/populationandmigration/populationestimates
34. Coats CJ, Gallagher MJ, Foley M, et al. Relation between serum N-terminal pro-brain natriuretic peptide and prognosis in patients with hypertrophic cardiomyopathy. Eur Heart J 2013;34:2529–2537
35. Wang S, Cui H, Ji K, et al. Impact of type 2 diabetes mellitus on mid-term mortality for hypertrophic cardiomyopathy patients who underwent septal myectomy. Cardiovasc Diabetol 2020;19:64
36. Neubauer S, Kolm P, Ho CY, et al.; HCMR Investigators. Distinct subgroups in hypertrophic cardiomyopathy in the NHLBI HCM Registry. J Am Coll Cardiol 2019;74:2333–2345
37. Watkins H. Time to think differently about sarcomere-negative hypertrophic cardiomyopathy. Circulation 2021;143:2415–2417
38. Dhandapany PS, Kang S, Kashyap DK, et al. Adiponectin receptor 1 variants contribute to hypertrophic cardiomyopathy that can be reversed by rapamycin. Sci Adv 2021;7:eabb3991
39. Gonzalez AB, Young L, Doll JA, Morgan GM, Crawford SE, Plunkett BA. Elevated neonatal insulin-like growth factor I is associated with fetal hypertrophic cardiomyopathy in diabetic women. Am J Obstet Gynecol 2014;211:290.e1–290.e7
40. Cecchi F, Olivotto I, Gistri R, Lorenzoni R, Chiriatti G, Camici PG. Coronary microvascular dysfunction and prognosis in hypertrophic cardiomyopathy. N Engl J Med 2003;349:1027–1035
41. Fumagalli C, Maurizi N, Day SM, et al.; SHARE Investigators. Association of obesity with adverse long-term outcomes in hypertrophic cardiomyopathy. JAMA Cardiol 2020;5:65–72
42. Larsen CM, Ball CA, Hebl VB, et al. Effect of body mass index on exercise capacity in patients with hypertrophic cardiomyopathy. Am J Cardiol 2018;121:100–106
43. Varnava AM, Elliott PM, Sharma S, McKenna WJ, Davies MJ. Hypertrophic cardiomyopathy: the interrelation of disarray, fibrosis, and small vessel disease. Heart 2000;84:476–482
44. Neubauer S, Horn M, Cramer M, et al. Myocardial phosphocreatine-to-ATP ratio is a predictor of mortality in patients with dilated cardiomyopathy. Circulation 1997;96:2190–2196
45. Tower-Rader A, Mohananey D, To A, Lever HM, Popovic ZB, Desai MY. Prognostic value of global longitudinal strain in hypertrophic cardio-myopathy: a systematic review of existing literature. JACC Cardiovasc Imaging 2019;12:1930–1942
46. Ellis J, Valkovič L, Purvis LAB, Clarke WT, Rodgers CT. Reproducibility of human cardiac phosphorus MRS (^{31} P-MRS) at 7 T. NMR Biomed 2019;32:e4095
47. Tyler DJ, Emmanuel Y, Cochlin LE, et al. Reproducibility of ^{31}P cardiac magnetic resonance spectroscopy at 3 T. NMR Biomed 2009;22:405–413